J. Membrane Biol. 150, 9–20 (1996)

The Journal of
Membrane
Biology

Small Inward Rectifying K^+ Channels in Coleoptiles: Inhibition by External Ca^{2+} and Function in Cell Elongation

G. Thiel, A. Brüdern, D. Gradmann
Pflanzenphysiologisches Institut der Universität, Untere Karspüle 2, D-37073 Göttingen, Germany

Received: 6 June 1995/Revised: 12 September 1995

Abstract. Plant growth requires a continuous supply of intracellular solutes in order to drive cell elongation. Ion fluxes through the plasma membrane provide a substantial portion of the required solutes. Here, patch clamp techniques have been used to investigate the electrical properties of the plasma membrane in protoplasts from the rapid growing tip of maize coleoptiles. Inward currents have been measured in the whole cell configuration from protoplasts of the outer epidermis and from the cortex. These currents are essentially mediated by K^+ channels with a unitary conductance of about 12 pS. The activity of these channels was stimulated by negative membrane voltage and inhibited by extracellular Ca^{2+} and/or tetraethylammonium-CI (TEA). The kinetics of voltage- and Ca^{2+}-gating of these channels have been determined experimentally in some detail (steady-state and relaxation kinetics). Various models have been tested for their ability to describe these experimental data in straightforward terms of mass action. As a first approach, the most appropriate model turned out to consist of an active state which can equilibrate with two inactive states via independent first order reactions: a fast inactivation/activation by Ca^{2+}-binding and -release, respectively (rate constants $>>10^3$ sec^{-1}) and a slower inactivation/activation by positive/negative voltage, respectively (voltage-dependent rate constants in the range of 10^3 sec^{-1}).

With 10 mM K^+ and 1 mM Ca^{2+} in the external solution, intact coleoptile cells have a membrane voltage (V) of -105 ± 7 mV. At this V, the density and open probability of the inward-rectifying channels is sufficient to mediate K^+ uptake required for cell elongation. Extracellular TEA or Ca^{2+}, which inhibit the K^+ inward conductance, also inhibit elongation of auxin-depleted coleoptile segments in acidic solution. The comparable effects of Ca^{2+} and TEA on both processes and the similar Ca^{2+} concentration required for half maximal inhibition of growth (4.3 mM Ca^{2+}) and for conductance (1.2 mM Ca^{2+}) suggest that K^+ uptake through the inward rectifier provides essential amounts of solute for osmotic driven elongation of maize coleoptiles.

Key words: Ca^{2+} block — Coleoptile growth — K^+ channel — Patch clamping — *Zea mays*

Introduction

Extension of plant cells is limited by mechanisms which achieve loosening of the cell walls but also by those processes which supply solutes for a sufficient turgor pressure to drive cell expansion (Cosgrove, 1986). The effects of extracellular ions to stimulate (monovalent cations) or inhibit (divalent cations) elongation of grass coleoptiles (Cooil & Bonner, 1957; Tagawa & Bonner, 1957), stress that ion-specific processes are involved either in the mechanism controlling wall loosening and/or in those supplying solutes for osmotic driven elongation. Interpretation of the cation effects on the background of ion interactions with wall-loosening mechanisms have focused on the differential ability of ions to soften (e.g., K^+) or stiffen (e.g., Ca^{2+}) the mechanical properties of the cell wall (Cooil & Bonner, 1957; Tagawa & Bonner, 1957) or on the effect of Ca^{2+} to promote wall loosening acidification (Cleland & Rayle, 1977).

The different effects of mono- and divalent cations on coleoptile elongation can also be explained on the basis of ion-specific modulations of solute uptake required to drive expansion. Net K^+ uptake into coleoptiles directly correlates with tissue elongation (Haschke & Lüttge 1973, 1975) and underlines that K^+ uptake is a major source for osmotica necessary for turgor mainte-

Correspondence to: G. Thiel

nance. Furthermore, judging from the sensitivity of V to the concentration of extracellular K^+ ($[K^+]_o$), the relative K^+ conductance of the plasma membranes of coleoptile cells is high and decreases as the concentration of external Ca^{2+} ($[Ca^{2+}]_o$) is increased (Nelles & Müller 1975; Nelles 1976). Hence, the stimulating effect of $[K^+]_o$ on elongation could be interpreted as result of increased K^+ uptake and a subsequent rise in turgor. The inhibition of growth by $[Ca^{2+}]_o$ would accordingly be caused by a reduction of K^+ uptake.

In the present investigation, we have studied the electrical properties of the plasma membrane of protoplasts from coleoptile cortex tissue and from the outer epidermis. The passive transport properties of the plasma membrane are dominated by an inward rectifying K^+ channel, which can serve — in conjunction with an energizing H^+ ATPase — as device for K^+ uptake. We found similar inhibitory constants of $[Ca^{2+}]_o$ in the millimolar range both for growth inhibition and for K^+-inward conductance. This finding supports the idea that $[Ca^{2+}]_o$ inhibits cell elongation of coleoptiles by blocking the main pathway for K^+ uptake in osmotically relevant amounts.

To understand the crucial experimental data of inward K^+ currents on physiological grounds, their characteristics with respect to $[Ca^{2+}]_o$ dependency and time course of voltage-dependent changes in activity have been analyzed in more detail. As a first approach, the data are consistently described by a straightforward mass action model (with a unique set of parameters) for activation/inactivation kinetics of the main K^+ conductance with respect to $[Ca^{2+}]_o$, V and time.

Materials and Methods

Protoplast Preparation

Protoplasts from the coleoptile of maize (cv, mutin; KWS Saatzucht, Einbeck, Germany) seedlings (4–6-days old) were prepared under conditions of minimalized proteolysis as described previously (Diekmann, Venis & Robinson, 1995). In short, 10-mm-long coleoptile tips were separated from the primary leaf and from the coleoptile apex (3–5 mm). The tissue was vacuum-infiltrated with the enzyme mixture for 15 min and then incubated for 3 hr on a shaker. The enzyme mixture contained 1.5% (w/v) cellulase Onozuka RS (Yakult Honsha, Tokyo, Japan), 0.1% (w/v) pectolyase Y-23 (Seishin, Tokyo, Japan), 0.5% (w/v) mazerozyme Onozuka R10 (Yakult Honsha, Tokyo, Japan), 10 mM Na-ascorbate, 2% (w/v) BSA-fraction 5 (Sigma) and 0.5 M sorbitol).

Electrical

Tight seal (1–10 GΩ), whole cell and single channel measurements were made as described by Hammil et al. (1981). Protoplasts were bathed in a solution containing (in mM): 500 sorbitol, 20 Mes (2[N-morpholino]ethanesulfonic acid) /KOH, pH 6.1, giving a K^+ concentration of 10. Different amounts of $CaCl_2$ were added as indicated. The standard pipette solution contained (in mM): 175 K-glutamate, 10 KCl, 5 $MgCl_2$, 4 Na_2-ATP, 150 sorbitol, 20 Hepes (N-[2-hydroxyethyl]piperazine-N′ethanesulfonic acid)/ KOH, pH 7.5 and 100 μM EGTA. The reference electrode (filled with same electrolyte as patch electrode) was connected with the bath *via* a salt bridge (100 mM KCl in 2% Agar).

Liquid junction voltages were determined for individual combinations of solutions and *V*s corrected accordingly (Neher, 1992). For the calculation of equilibrium voltages and cytoplasmic activities the activity coefficients given by Robinson and Stokes (1968) were taken into account.

Whole cell and single channel currents were measured with an EPC-7 amplifier (List Electronic, Darmstad, FRG) interfaced (Tl-1 DMA interface) with an analog digital converter and recorded directly on a microcomputer (sampling rate 400 Hz for whole cell currents, 5 kHz for single channel currents). Data acquisition and clamp voltage control was obtained through a microcomputer via the pCLAMP hardware and software facilities (Axon Instruments, Foster City, CA). The membrane voltage of protoplasts was measured with the patch clamp amplifier in the current clamp mode ($I = 0$) immediately after achieving the whole cell configuration. To measure V of intact coleoptile cells, coleoptile segments (without primary leaf and apex) were mounted horizontally in a perspex chamber after preincubation on distilled water for 1 hr. Cells of the outer epidermis were impaled with a conventional microelectrode containing the same solution used in patch electrodes for whole cell measurements (*see* above). A reference electrode containing the same electrolyte as the voltage recording electrode was connected via a salt bridge (100 mM KCl in 2% Agar) with the bath. The electrodes tip-potential in the bath solution (about −10 mV) was compensated to zero before impalement. The voltage between the cell interior and a reference electrode in the external perfusion solution (in mM: 20 Mes /KOH, pH 6.1 and 1 $CaCl_2$) was recorded with a voltage amplifier (μP, Wye Science, UK).

Protoplast diameters were measured with an eyepiece micrometer, and the surface area was calculated assuming a spherical shape.

Coleoptile Elongation

Approximately 10-mm-long segments of the coleoptile tip were isolated in the same way as for protoplast preparation. After gently abrading the cuticle with diatomaceous earth, 5 segments per treatment were thread on a stainless steel rod and stored for 1 hr in distilled water for depletion of endogenous auxin. Following this preincubation, segments were transferred to the test medium (15 ml) containing 2 or 10 mM K-acetate (titrated with acetic acid to pH 5) and tetraethylammonium-Cl (TEA) or different concentrations of $CaCl_2$. For elongation measurements, coleoptile cylinders were magnified 30 times on an overhead projector and the projection measured directly before and 6 hr after incubating coleoptiles in test solution in the dark on a shaker.

Models Used

The chord conductance (activity) of the investigated K^+ inward rectifier is voltage-sensitive per definition and turned out to be inhibited by $[Ca^{2+}]_o$. These qualitative properties can be expressed by three different models of mass action which can be distinguished quantitatively:

Parallel: $I_c - A - I_v$

Serial1: $A - I_c - I_{Cv}$

Serial2: $A - I_v - I_{vC}$

Here A means the active form of the K^+ transporter with a maximum linear conductance G_{max}; I_C is the inactive form which results

from binding of Ca^{2+} to the active form: thus $I_C = A[Ca^{2+}]/K_{IC}$, with K_{IC} being the inhibition constant for inactivation by Ca^{2+}; correspondingly, I_v is the inactive form which results from the voltage-sensitivity, where the *c*oefficient for the (exponential) effect of *v*oltage is $C_v = \exp(du)$ with d being a weighting factor for the normalized membrane voltage $u = VF/(RT)$, where R, T and F have their usual thermodynamic meanings. Thus $I_v = AC_v/K_{Iv}$ with K_{Iv} being the inhibition constant for inactivation by voltage. In the *serial model* 1 the Ca^{2+}-blocked state I_C can be converted into another inactive state I_{CV} by a voltage–sensitive transition. Correspondingly, the voltage inhibited state I_V in *serial model* 2, can change into another inactive state I_{VC} by Ca^{2+} binding. In these terms, the steady-state conductances of the three models are:

$$\textit{Parallel: } G = G_{max}/(1 + [Ca]/K_{IC} + C_V/K_{IV}) \quad (1a)$$

$$\textit{Serial1: } G = G_{max}/(1 + [Ca]/K_{IC}(1 + C_V/K_{IV})) \quad (1b)$$

$$\textit{Serial2: } G = G_{max}/(1 + C_V/K_{IV}(1 + [Ca]/K_{IC})) \quad (1c)$$

Since in our first approach d did not turn out to differ significantly from 1, it will be more convenient in several places to substitute the expression C_V/K_{IV} by $\exp(u - u')$, where $u' = \ln(K_{IV})$.

For the description of the time course of the current changes upon voltage steps, individual rate constants k_A for activation and k_I for inactivation have to replace the equilibrium constants $K_I = k_I/k_A$. In our case, the rates for Ca^{2+}-binding and debinding were too fast to be resolved in time; thus, only the voltage-sensitive reactions k_I and k_A were reflected in the main current relaxations which could be described with one single exponential due to the conductance change $G(t) = G_0 + \Delta G(t)$, where G_0 is the steady-state conductance before the voltage step, $\Delta G(t) = \Delta G_\infty(1 - \exp(kt))$, $\Delta G_\infty = G_\infty - G_0$ is the difference between the final steady-state conductance G_∞ and G_0, and the velocity constant $k = k_I + k_A$. Thus, upon a voltage step from V_0 to V, the time course of the current through a transporter with the equilibrium voltage E would be $I(t) = I_0 + (V - V_0)\,\Delta G(t)$, where $I_o = G_0(V_0 - E)$ is the steady-state current at V_o. The target voltage V determines not only the new $G = G_{max}/(1 + k_I/k_A))$ but also the velocity constant $k = k_I + k_A$ of the relaxation.

Voltage-sensitivity enters the system by the expressions $k_I = k_I^0 \exp(d,u)$ and $k_A = k_A^0 \exp(d_A u)$, where the superscript ^{0} denotes the value of the respective rate constant at zero voltage. The weighting factors $d_A = zn\Delta\delta$ and $d_I = zn\Delta(\delta - 1)$ comprise the number, n, of moved particles with the charge z, which overcome an Eyring barrier during the switching process; the peak of the Eyring barrier is located at the distance δ ($0 < \delta < 1$) of the effective fraction Δ ($0 < \Delta < 1$) of the voltage drop across the membrane. The fits did not significantly improve for ds different from $d_I = 0.5$ and $d_A = -0.5$. This can be attributed to a symmetric Eyring barrier ($\delta = 0.5$) and simple unity for z, n, and Δ, although larger (integer) values of z and/or n with a corresponding smaller Δ are possible, if not even more likely.

Numerical Procedures

For analysis of a full experiment, typically 14 current traces of 2-sec duration with sampling intervals of 0.0025 msec (800 data points) were available for 4 different $[Ca^{2+}]_o$. Steady-state currents were taken from at least 10 data points at the end of a trace after at least five times of the relaxation time had passed.

For computing economy in fitting the time courses of the currents, the 800 data points per tracing have been reduced to 17 in a logarithmic scale, taking the first two data points individually, the second ones as means of two original current readings, the third two reduced points as means of four original points and so on. Data points during about the first msec (6 data points) have been omitted for the fits because they were usually contaminated with an uncompensated fraction of capacitive currents. For presentation purposes, the original data points are shown by their full number, and the fitted curves start from time zero.

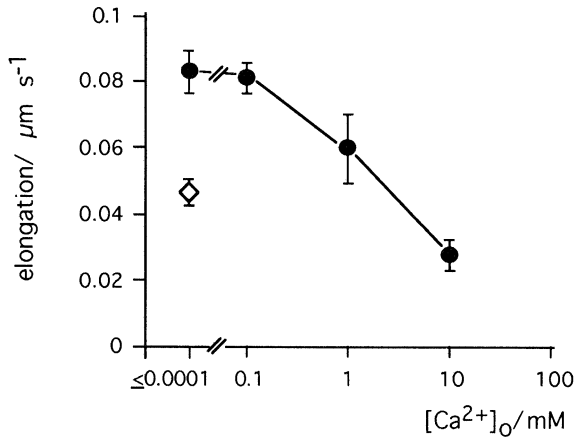

Fig. 1. Effect of $CaCl_2$ and TEA on elongation of abraded maize coleoptile segments. After preincubation for 1 hr in dest. water, segments were incubated in 10 mM K-acetate buffer, pH 5 without (<0.0001 mM) or with addition of various concentrations of $CaCl_2$ (●) or 20 mM TEA (◇). Rate of elongation determined from the difference in coleoptile length before and after 6 hr in acid medium. Mean ± SD of 4 experiments.

Results

Coleoptile Elongation

Elongation of abraded and auxin-depleted maize coleoptile segments in acidic medium was measured in responds to extracellular $CaCl_2$ and TEA. Figure 1 shows that $[Ca^{2+}]_o \geqslant 1$ mM inhibits segment elongation in a concentration dependent manner. Adding 10 mM $CaCl_2$ to a nominally $[Ca^{2+}]_o$ free solution decreases the rate of elongation to 34% in 10 mM K-acetate solution. Elongation of coleoptile segments was also inhibited when the K^+ channel inhibitor TEA was added (20 mM) to the nominally $[Ca^{2+}]_o$ free test solution. The remaining rate of elongation was 45% compared to the control.

Membrane Voltage of Intact Coleoptile Cells and of Protoplasts from Maize Coleoptiles

To measure V of intact coleoptile cells, cells of the outer epidermis were impaled with a conventional voltage recording electrode. In a bathing solution containing 10 mM K^+ and 1 mM Ca^{2+} a stable V of −105 ± 7 mV (number of experiments, $N = 5$, ± SD) was measured. For comparison, V was also measured in protoplasts immediately after achieving the whole cell configuration. In 18 protoplasts bathed in a solution also containing 10

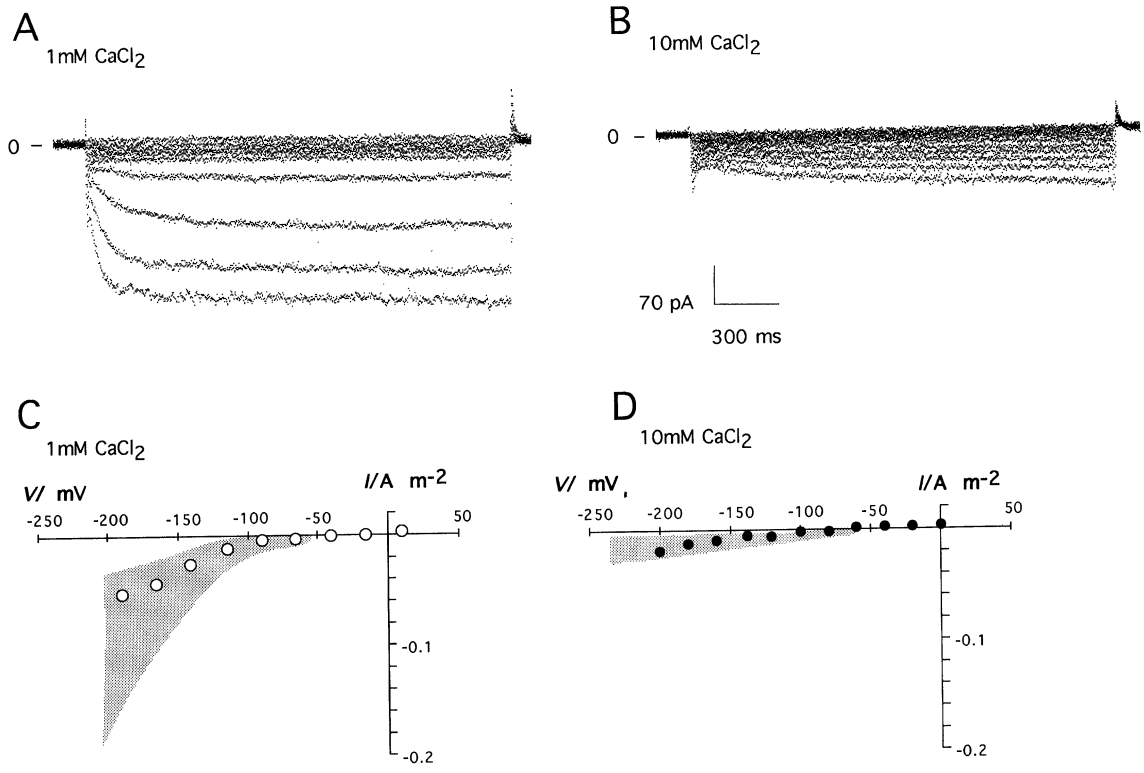

Fig. 2. Effect of extracellular $CaCl_2$ on whole cell inward currents and steady-state current-voltage relations in protoplasts from maize coleoptiles. Currents elicited by hyperpolarizing steps in protoplasts from the outer epidermis bathed in standard solution (in mM): 500 sorbitol, 20 Mes/KOH pH 6.1 containing either 1 mM (*A*) or 10 mM (*B*) $CaCl_2$. Text voltages ranged from +10 to −190 mV (*A*) or from 0 to −200 mV (*B*) from a holding voltage of −5 mV; current zeros indicated on left. (*C,D*) steady-state *I/V* relations from current recorded at end of the test pulses (mean over final 50 msec at test voltages) in *A* (○) and *B* (●). Shaded areas represent standard deviation of steady-state *I/V* relations obtained from nonspecified protoplasts in 1 mM $CaCl_2$ (*C*) ($N = 13$) or 10 mM $CaCl_2$ (*D*) ($N = 10$). Mean currents obtained by linear interpolation of individual *I/V* plots.

mM K^+ and 1 mM Ca^{2+} (compare intact cells) a mean V of −53 ± 22 mV (range: −33 to −121 mV) was measured.

Whole Cell Membrane Currents

Figure 2 *A,B* shows membrane currents (*I*) of two protoplasts from the outer epidermis of maize coleoptiles. In these cases an anatomical identification of the protoplasts was possible because of visible anthocyanin red staining of the vacuoles. In cross-sections of maize coleoptiles such anthocyanin stained vacuoles are present only in the outer epidermis. When bathed in experimental solution containing low $CaCl_2$ (here 1 mM) negative steps of clamp voltages evoked a dual current response. An instantaneous current response was followed by a slow rising second component. In the present case (Fig. 2*A*), the time for half maximal current of the slow response was 135 msec at −140 mV and decreased with negative V to 79 msec at −190 mV. The overall steady-state current/voltage (*I/V*) relation (including both components) is characterized by pronounced inward rectification (Fig. 2*C*). Another example is treated below in more detail.

When protoplasts from the outer epidermis were bathed in the same solution but containing high $CaCl_2$ concentrations (here 10 mM) the inward current was much smaller; in particular the slowly rising inward current seen in low $CaCl_2$ was absent. The resulting steady-state *I/V* relation was essentially linear over the V range tested.

The sensitivity of the inward current to V and $[Ca^{2+}]_o$ was characteristic for all the protoplasts from coleoptiles investigated. The standard deviation of the steady-state currents ($V \leqslant -60$ mV) from the bulk of anatomically nonspecified protoplasts tested is shown as shaded area in Fig. 1 *C* and *D*. The electrical characteristics of the classified epidermis protoplasts fall into the range of the *I/V* relations obtained for the bulk of the protoplasts investigated in low and high $CaCl_2$ (Fig. 1; Table 1). Some of the nonspecified protoplasts contained proplastids. Because proplastids are present in cortex cells of the coleoptile but not in epidermis cells (Hinchman, 1972), protoplasts with visible proplastids were considered to originate from the cortex. Comparing the inward conductances (in 1 and 10 mM $CaCl_2$) of these protoplasts with those from epidermis protoplasts

Table 1. Impact of extracellular Ca^{2+} concentration ($[Ca^{2+}]_o$), of cell type and of the concentration of the Ca^{2+} buffer EGTA in pipette medium on membrane conductance

Pipette:	100 μM EGTA						4 mM EGTA
Cell type:	Nonspecified		Outer epidermis		Cortex		Nonspecified
Column	A	B	C	D	E	F	G
$[Ca^{2+}]_o$/mM	1	10	1	10	1	10	10
G/Sm^2	0.96 ± 0.8	0.12 ± 0.08	0.86 ± 0.37	0.15 ± 0.14	0.75 ± 0.78	0.14 ± 0.09	0.09 ± 0.07
N	13	10	4	3	5	4	3
Significance/ %		B = A: 98	C = A: 20	D = B; 37	E = C: 19	F = D: 8	G = B: 39

Conductance ($G = (i_{-180\ mV} - i_{-70\ mV})/110$ mV) measured from cells bathed (in mM): 500 sorbitol, 20 Mes/KOH pH 6.1 with either 1 or 10 $CaCl_2$ in external solution. Currents determined by linear interpolation from *I/V* plots. Data grouped by cell types: outer epidermis (anthocyanin red stained protoplasts; column *C,D*), cortex (protoplasts with proplastides, column *E,F*) and nonspecified cells (cells without anthocyanin red staining including cortex cells; column *A,B,G*). Conductance obtained either with 100 μM or 4 mM EGTA in pipette solution. For selected pairs of interest the confidence limit (in % from Student *t*-test) is given for hypothesis that two columns are different.

showed no significant difference between both protoplast types (Table 1).

K^+ Selectivity of Inward Rectifier

To determine the substrate of the inward rectifier, the whole cell currents were measured in the presence and absence of the K^+ channel inhibitor TEA in the external solution. Figure 3 shows that the slow rising inward current obtained in the absence of the inhibitor was abolished in the presence of the K^+ channel inhibitor leaving an essentially linear, background conductance.

For determination of the reversal voltage of the inward rectifier, tail current relaxations were recorded (Fig. 4). For this procedure, the inward rectifier was first activated by 1.5-sec-long voltage steps to −180 mV in solutions containing 10 and 50 mM K^+. In subsequent deactivating voltage steps the current relaxation was determined as the difference between the current just after start of the deactivating voltage step and the steady-state current reached within 1 sec. These tail currents reversed at −63 ± 12 mV ($N = 7$) in 10 mM K^+ and −25 ± 2 mV ($N = 3$) in 50 mM K^+. For comparison, the Nernst K^+ reversal voltages calculated from the cytoplasmic K^+ activity (131 mM, activity coefficient, δ: 0.73) is −67 mV and −29 mV for an extracellular K^+ activity of 9.5 mM (δ: 0.95) and 42 mM K^+ (δ: 0.84) respectively.

Inward Rectifier and Time-averaged *I/V* Relation of Single Channel Currents

Figure 5 shows traces of single channel current fluctuations in the plasma membrane of coleoptile protoplast recorded in the cell attached configuration with 140 mM KCl, 5 mM Hepes/KOH, pH 7.5 as pipette electrolytes. To determine the unitary open channel conductance and

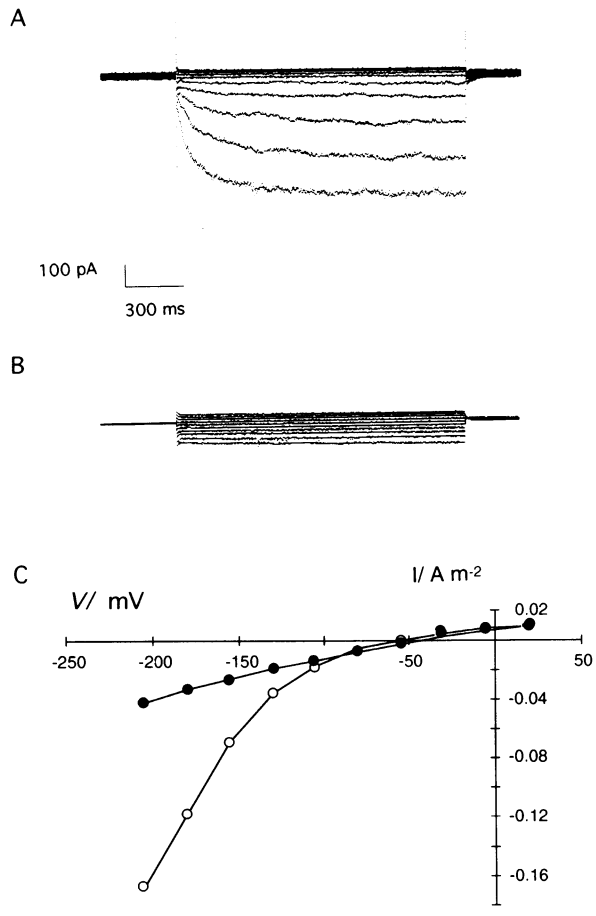

Fig. 3. Inhibition of inward rectifier by extracellular TEA. Whole cell inward currents elicited in absence (*A*) and presence (*B*) of 20 mM TEA in extracellular solution (mM: 500 sorbitol, 20 Mes/KOH pH 6.1, 1 $CaCl_2$ and 40 K-gluconate) by clamping the membrane to voltages between +20 and −205 mV from −55 mV as holding voltage. Steady-state *I/V* relation (mean over final 50 msec at test voltages) in absence (○) and presence (●) of TEA plotted in *C*.

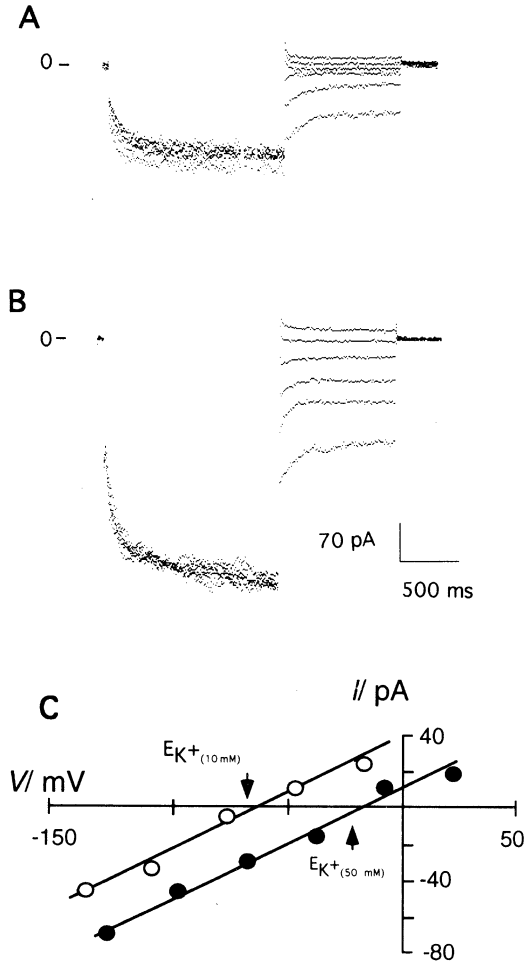

Fig. 4. Deactivation ('tail' currents) current-voltage relation in 10 and 50 mM K^+. Tail currents recorded in whole-cell mode in protoplasts form maize coleoptiles bathed (in mM): 500 sorbitol, 20 Mes/KOH pH 6.1 (*A*, 10 K^+) and after addition of 40 K-gluconate (*B*, 50 K^+). Inward rectifier first activated by 1.5-sec long voltage steps to −180 mV and subsequently deactivated at test voltages between −17 and −137 mV (*A*) and between +22 and −128 mV (*B*). Current relaxation between current just after start of the deactivating step and the steady-state current reached within 1 sec are plotted in (*C*) for 10 mM K^+ (○) and 50 mM K^+ (●).

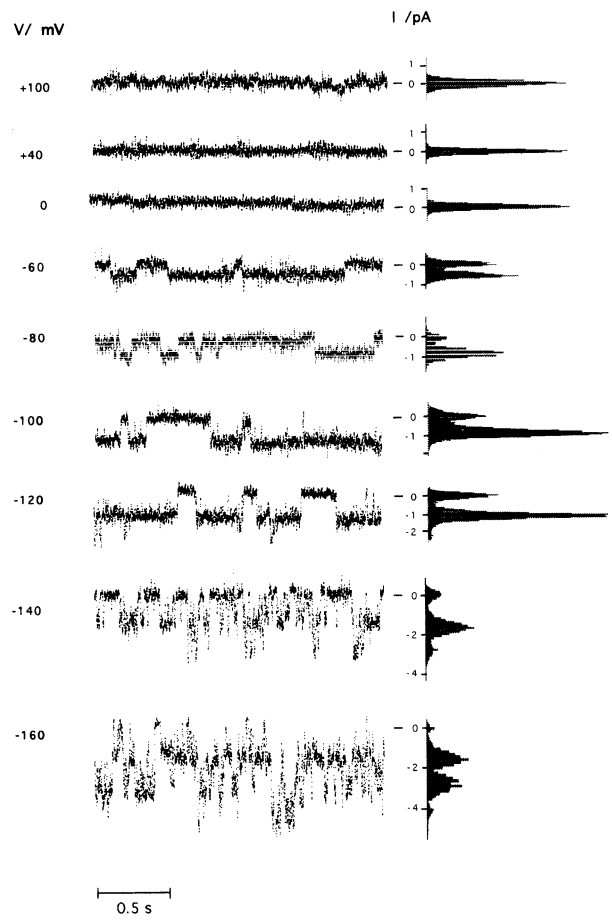

Fig. 5. Single channel currents with unitary conductance of 12 pS underly K^+ inward rectifier. Stimulating effect of negative *V* on activity (left panel). Channel activity in the plasma membrane measured in cell-attached configuration (pipette solution, in mM: 140 KCl, 5 Hepes/KOH, pH 7.5, protoplast bathed in 500 sorbitol, 0.5 $CaCl_2$ and 20 Mes/KOH pH 6.1). Membrane voltage (numbers on the left) as the sum of holding voltage and *V* of the protoplasts, measured at the end of channel recording upon achieving whole cell configuration. All point histograms (right panel) obtained from 10-sec long recordings at test voltages. Peaks around 0 pA represent baseline noise (= time with all channels closed). Other peaks represent the open channel current for up to 3 channels open. Numbers on the right common scaling for channel current recordings and histograms with 0 for channels closed.

the open probability at different voltages all-point histograms were plotted from 10-sec-long current recordings (Fig. 5 right panel). With a minimum of three channels of the same conductance present in the patch the histograms were fitted by ≤4 Gaussians. The unitary open channel current was obtained from the difference between the distribution peaks. The open probability, P_o, was calculated from the relative areas of the Gaussians assuming three channels in the patch (Bertl & Slayman, 1990). The data for the unitary open channel current and for the open probability are plotted in Fig. 6. The linear *I/V* relation of the open channel currents (12 pS conductance) extrapolates to a reversal voltage of about −15 mV. Such an extrapolated reversal voltage would be measured for a K^+ permeable channel if the cytoplasmic K^+ activity was 178 mM.

A time-averaged open channel current (unitary open channel current $*P_o$) reflects the steady-state whole-cell current-voltage relation obtained in low $[Ca^{2+}]_o$ (Fig. 6). The time-averaged open channel *I/V* relation can be described with the same function and parameters used to fit the steady-state *I/V* curve from whole cell currents (Model *parallel a, see below*, Fig. 7).

Current Inhibition by Ca^{2+}

To test whether the inhibition of the K^+ inward rectifier in high $CaCl_2$ was due to $[Ca^{2+}]_o$ or Cl^-, $[Ca^{2+}]_o$ was

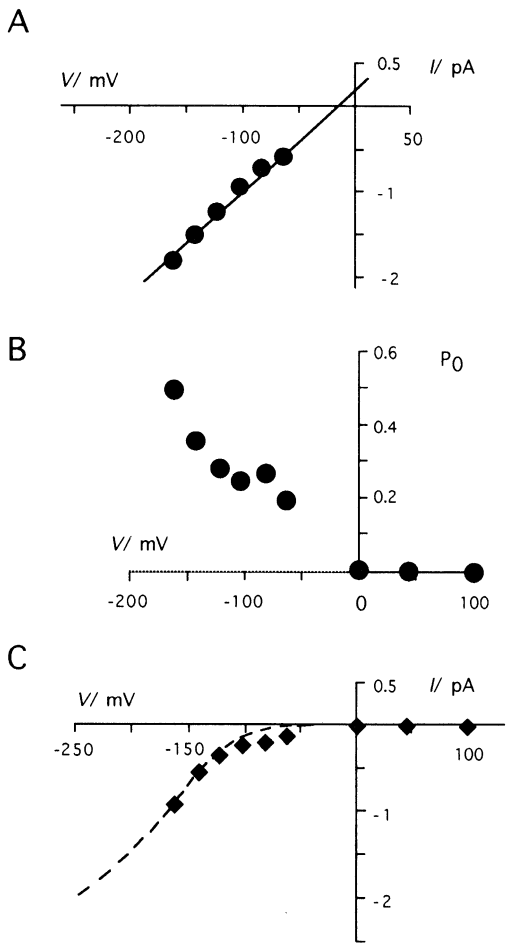

Fig. 6. Single channel current-voltage relation, open probability-voltage relation and time averaged open channel whole cell relation of cell-attached single channel measurements. From the Gaussian distributions of all point histograms (Fig. 5) the open channel current (*A*) was determined as the difference between the peak means of closed and open channel current distribution. Open probability (*B*) determined from relative areas under the Gaussians corresponding to closed state and open levels of 3 channels in the patch. The time averaged *I/V* relation (*C*) obtained as product ($I^* P_o$) of the open channel current in *A* and the open probability in *B*. The line in (*C*) is drawn according to model *parallel* a with a gating voltage $V_{ga} = -156$ mV (*cf.* Table 3).

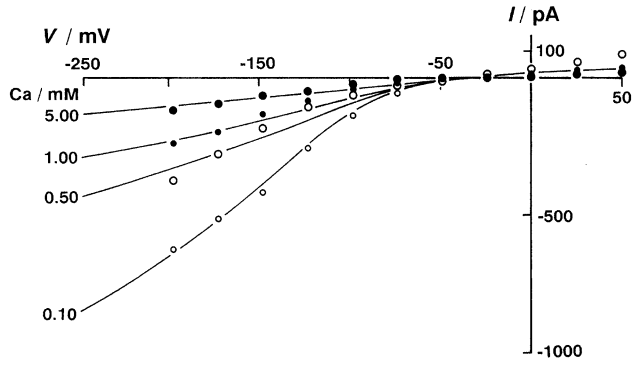

Fig. 7. Steady-state *I/V* curves of plasma membranes of coleoptile protoplasts exposed to various concentrations of Ca^{2+} in the bath. Example of measurements and fits; external solution (in mM): 0.1–5.0 $CaCl_2$ as marked, plus 500 sorbitol, 20 Mes/KOH pH 6.1 (= 10 K^+); points measured in whole cell configuration as steady-state currents upon voltage steps from holding voltage of −30 mV; curves fitted by parallel model a with fixed $d_V = 1$ and $d_C = 0$, plus fitted $G_{max} = 4.9$ nS, $G_b = 0.4$ nS, $V_{ga} = -121$ mV, and $K_{IC} = 0.24$ mM Ca^{2+}; MEAN $|I_{MEAS} - I_{FIT}| = 24$ pA.

increased in one protoplast from 0.5 to 5 mM by adding Ca-gluconate instead of $CaCl_2$. The resulting inhibition was comparable to that obtained in $CaCl_2$; it shows that $[Ca^{2+}]_o$ is responsible for the effect (Fig. 9).

Inhibition of the inward rectifier by extracellularly added Ca^{2+} could be due to a direct Ca^{2+} block from the extrafacial side. Alternatively, Ca^{2+} may act from the cytoplasmic side as a consequence of an indirect increase of cytoplasmic Ca^{2+} activity. To test the latter possibility, the internal Ca^{2+} buffer concentration was increased by adding 4 mM instead of 100 μM EGTA to the pipette solution. With this higher concentration of the Ca^{2+} chelator EGTA in the pipette solution the total Ca^{2+} concentration in the cytoplasm would have to increase 24 times more in order to produce a rise in Ca^{2+} activity comparable to that with the low buffer concentration (Föhr et al., 1992). Protoplasts dialyzed for more than 20 min with the higher Ca^{2+} buffer concentration in the pipette showed in 10 mM $[Ca^{2+}]_o$ the same linear *I/V* relation as those tested with the lower buffer concentration (*not shown*). There was no significant difference in the conductance measured in cells with different Ca^{2+} buffer load (Table 1).

KINETICS

The observed phenomena of $[Ca^{2+}]_o$-modulated inward conductance for K^+ have been analyzed in reaction kinetic terms. For the superposition of the effects of $[Ca^{2+}]_o$ and *V*, three models have been introduced in Materials and Methods. These three models have been subdivided again (submodel *a-c*), with respect to the degree of voltage-sensitivity.

Submodel *a* reflects the simplest situation with a symmetric Eyring barrier ($\delta = 0.5$) over the entire membrane voltage ($\Delta = 1$), for the voltage-sensitive gating reaction of movement of one ($n = 1$) particle with the charge number +1 ($z = 1$); in this model $d_A = -0.5$ and $d_I = -0.5$ ($d_I - d_A = d_V = 1$) are fixed numbers, resulting in an ''Nernstian'' conductance change by a factor 10 per 59 mV voltage change.

In submodel *b*, this relationship ($d_V = 1$) is not fixed; but sub- and super-Nernstian slopes are allowed. Although this model appears to be more realistic, it did — compared to model *a* — not provide a significantly improved description of the data.

Table 2. Resulting global errors from fitting various models to 4 sets of *I/V* curves recorded with different $[Ca^{2+}]_o$

Model	Mean deviation /% ± SD	d_v	d_C
Parallel:			
I_C-*A*-I_V			
a	100 ± 20	1.0	0
b	113 ± 13	1.0 ± 0.4	0
c	107 ± 27	1.0	0.11 ± 0.07
Serial1:			
A-I_C-I_{CV}			
a	167 ± 100		
b	213 ± 127		
c	227 ± 127		
Serial2			
A-I_V-I_{VC}			
a	260 ± 33		
b	173 ± 80		
c	213 ± 87		

Mean deviations (in % ± SD) related to 100% of result of model parallel *a*; d_V and d_C are exponential coefficients in expressions e^{du} to describe voltage-sensitivity of voltage-gating and of Ca^{2+}-gating respectively; $u = VF/(RT)$.

Submodel *c* was used to examine whether the Ca^{2+} block has a voltage-sensitivity of its own, of the form $I_{CV} = A[Ca^{2+}]\exp(d_C u)/K_{IV}$. In the corresponding fits, d_V was fixed to 1.0 and d_C was allowed to vary.

The nine models were fitted to each set of *I/V*-curves from an individual protoplast by a least-squares procedure yielding a mean deviation $I_{MEAS} - _{FIT}$, as a measure for the quality of the fits. Free parameters were the two inhibition constants K_{IC} and K_{IV} for the effects of $[Ca^{2+}]_o$ and *V*, a maximum conductance G_{max} of the main K^+ transporter under investigation, a background conductance G_b, d_V in models *b* and d_C in models *c*. For the global analysis of all data sets from protoplasts of various size, G_{max} was related to G_b by the a ratio $R = G_{max}/G_b$. For evaluation of the fits, the relative errors were multiplied by the number of free parameters (three for model *a*, namely K_{IV}, K_{IC} and *R;* and four for models *b* and *c* where d_V respectively d_C were fitted in addition). These products served as a measure for the quality of the model description, and were related to the best case (model *parallel a:* 100%). It should be mentioned, that for the fits the equilibrium voltage of the background conductance, E_b, was usually fixed at the resting voltage (V_r about −40 mV), and that fits with a floating E_b did not result in a better description but converged to $E_b \approx V_r$ with an accuracy of 10 mV.

The results of the global analysis are listed in Table 2, and can be summarized as follows: (i) The *parallel* model is more appropriate throughout (small mean errors and little variation) than either of the two serial models (about 2-fold mean errors and much wider variation). (ii) Therefore, a reasonable discussion of the submodels *a*, *b* and *c* can only apply for the *parallel* model. (iii) Comparison of *parallel a* and *parallel b* shows, that a free d_V as an additional fit parameter (submodel *b*) does not improve the quality of the fit compared with a fixed $d_V = 1$ (submodel *a*); therefore $d_V = 1$ can be taken as fair approximation at this level of analysis. (iv) With the model *parallel c*, the resulting d_C does not differ significantly from zero; hence, the assumption of voltage-gated Ca^{2+} block is not supported by the results, and the simplest model *parallel a* (with three fitted parameters) can be used as a good approach.

An example of a set of experimental steady-state data and fitted curves using the model *parallel a* is shown in Fig. 7; the numerical model parameters for this example are given in the legend to Fig. 7. Average parameters from these steady-state kinetics are listed in Table 3 together with an example of absolute rate constants for voltage-controlled activation (k_A) and inactivation (k_I), as obtained by fitting the time courses of the current responses upon negative voltage steps (Fig. 8).

In principle, the model with the fitted parameters describes not only the activation kinetics of the inward rectifier upon negative voltage steps but also the time course of the inactivation upon positive voltage steps. Traces of these kinetics can be identified in Fig. 8 in the upper left corner, where the fitted curves for positive voltage steps (e.g., from the holding voltage −40 to +90 mV) display fast relaxations, $I(t) = I_o\, e^{-kt}$, e.g., for a step from $V' = -40$ mV to $V = 90$ mV with $k_{(90\ mV)} = k_{A(90\ mV)} + k_{I(90\ mV)} = k_A{}^0 e^{-u/2} + k_I{}^0 e^{u/2} = (0.45/5.8 + 130 * 5.8)\text{sec}^{-1} = 753\ \text{sec}^{-1}$, corresponding to a time constant $\tau = 1/k$ of 1.3 msec and a small current amplitude $I_0 = A_{(-40\ mV)} G_{max}(V - V')$, with $A_{(-40\ mV)} < 0.01$. These current relaxations (''tail currents'') are too small to be resolved in the measurements with the much larger capacitive current transients superimposed.

Fits of the analyzed current relaxations for activation might look much nicer, if each tracing had been described by an individual exponential function with its own set of coefficients; however, the large number of fitted parameters would render such an approach inferior to our approach of describing as many as possible phenomena by as few as possible model parameters. In this context, it should be mentioned, that in high concentrations (about 10 mM) of $[Ca^{2+}]_o$, the inward currents were too small to be fitted well by the simple model within an entire ensemble of *I/V* curves from (lower) $[Ca^{2+}]_o$. Since these deviations point to extra processes which are not investigated here (i.e., Ca^{2+} induced inhibition of background conductance), the corresponding data (which are not very impressive anyway because of their insignificant amounts) are not shown here in detail.

Correlation between Ca^{2+}-evoked Block of K^+-inward Rectifier and Coleoptile Elongation

To compare the Ca^{2+}-evoked inhibition of the inward rectifier and the Ca^{2+}-evoked inhibition of coleoptile

Table 3. Fitted parameters of model *parallel* a for dynamic- and steady-state kinetics of $[Ca^{2+}]_o$- and *V*-controlled K^+ channel

$Ae^u/K_{IV} = I_V \underset{k_I}{\overset{k_A}{\rightleftarrows}} A \overset{Ca^{2+}}{\leftrightarrow} I_C = A[Ca^{2+}]/K_{IC}$					
From relaxation fit (Fig. 8): rate constants for slow					
activation	$k_A = k^A * exp(d_A u)$;	k_A^O:	0.45 sec^{-1};	d_A:	−0.5
inactivation	$k_I = k_I^o * \exp(d_I u)$;	k_I^o:	130.5 sec^{-1};	d_I:	+0.5
Resulting inhibition constant for voltage-gating:					
$I_V = A(k_I^O/k_A^O)\exp((d_I - d_A)u) = \exp(du)/K_{IV}$:		K_{IV}:	0.0035;	*d*:	*1*
Corresponds to Gating voltage $V_{ga} = (RT/F)\ln(K_{IV})$:		V_{ga}:	−142 mV		
From $n = 4$ sets of steady-state *I/V* curves with different $[Ca^{2+}]_O$ (*cf.* Table 2)					
Mean gating voltage corresponds to inhibition constant for voltage gating		V_{ga}:	156 ± 30 mV		
$K_{IV} = \exp(V_{ga}F/(RT))$;		K_{IV}:	0.002*/3.3		
Mean inhibition constant K_{IC} for Ca^{2+} inhibition		K_{IC}:	1.5*/4.5 mM		
Mean of maximum K^+ inward conductance		G_{max}:	6.5 ± 3.3 nS		
Mean ratio $R = G_{max}/G_{Leak}$:		*R*:	7.4 ± 3.4		

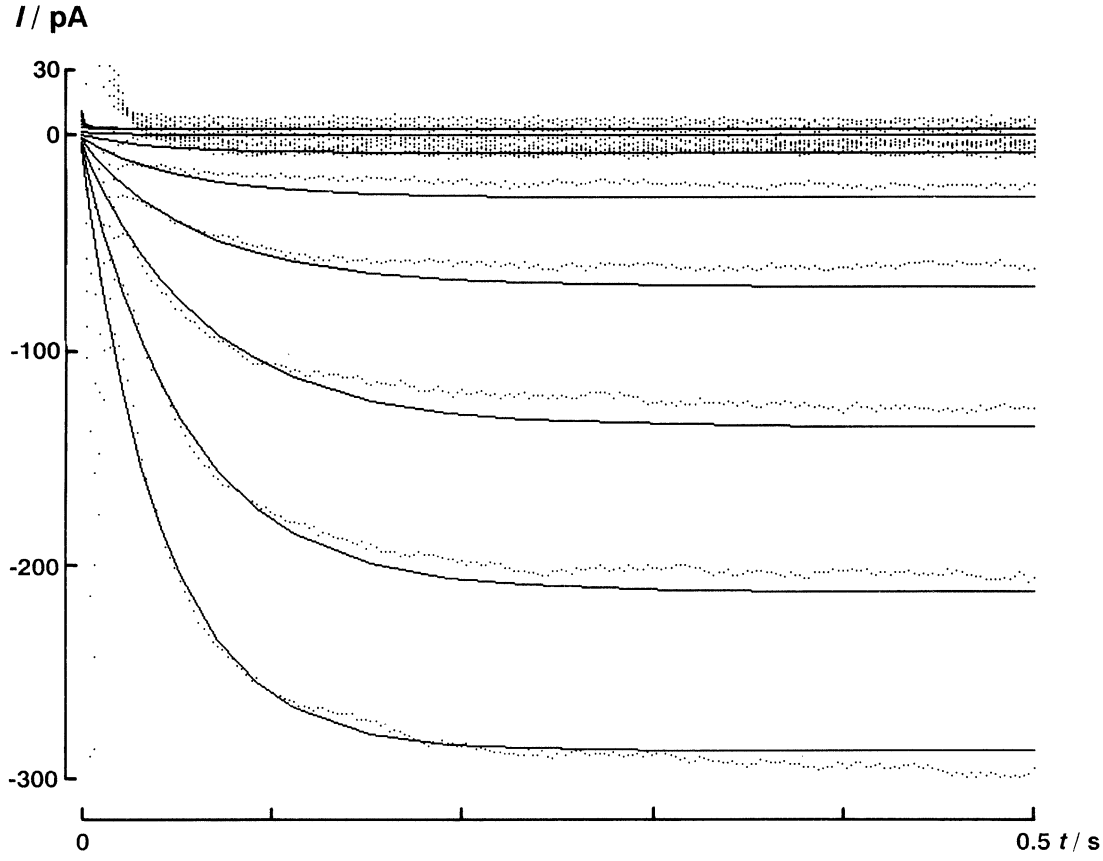

Fig. 8. Current-relaxations upon voltage steps on the plasma membrane of coleoptile protoplasts; example of measurement and fits; external solution (in mM): 1.0 $CaCl_2$, 500 sorbitol, 20 Mes/KOH pH 6.1; points: measured in whole-cell configuration as relaxations upon voltage steps from a common start voltage (−50 mV holding/resting voltage) to various target voltages (from 90 to −190 mV in 20 mV increments); curves: fits by model *parallel* a with fixed $d_V = 1$ and $d_C = 0$, plus fitted $G_{max} = 2.7$ nS, $G_b = 0.8$ nS, $k_A^0 = 0.05$ sec^{-1}, $k_I^0 = 13$ sec^{-1}, and $K_{IC} = 7$ mM $[Ca^{2+}]_o$; mean $I/_{meas} - /_{fit}I = 11$ pA; experimental data from first 7 msec (capacitive transients) omitted for fits: background currents ($I_b = G_b(V\text{-}50$ mV) subtracted.

elongation, the membrane conductance at −130 mV — a voltage driving substantial current through the inward rectifier — and the rate of coleoptile elongation determined over 6 hr in acidic solution with 10 mM K-acetate were normalized for data at 1 mM $[Ca^{2+}]_o$. A plot of the normalized data (Fig. 9) shows a similar decrease of both parameters as a function of $[Ca^{2+}]_o$. The data sets were fitted by the Hill-equation:

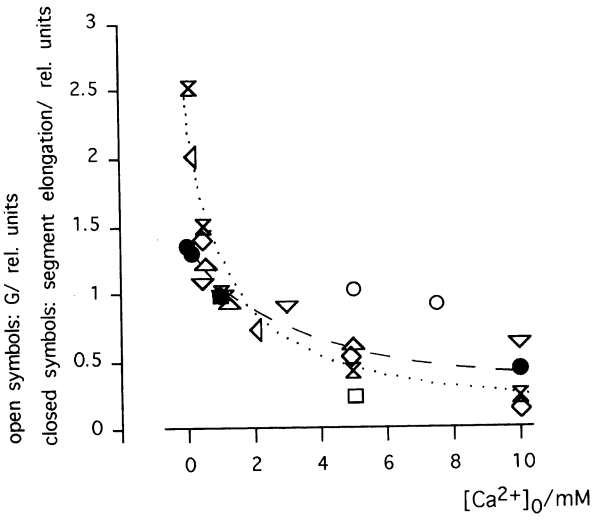

Fig. 9. Rate of coleoptile elongation and K^+-chord conductance at −130 mV as function of $[Ca^{2+}]_o$. Coleoptile elongation in 10 mM K-acetate (closed symbols), crossreference to data in Fig. 1 and K^+ conductance (*G*, open symbols) obtained from whole cell currents in protoplasts bathed in standard solution (in mM): 500 sorbitol, 20 Mes/KOH pH 6.1) as a function of Ca^{2+} added as Ca-gluconate (□) or $CaCl_2$ (remaining symbols). Different symbols represent different cells. Data normalized for values measured in 1 mM Ca^{2+}. Dashed and dotted lines from fitting data sets with Eq. 2 (*see* Results) yielding a half maximal inhibition for coleoptile elongation and for *G* in 4.3 mM and 1.2 mM $[Ca^{2+}]_o$ respectively.

$$a = a_{\max}\,1 - \left(\frac{1}{1 + (K^*_{IC}/[Ca^2]_o)^r}\right) \qquad (2)$$

yielding a maximal rate, a_{max}, of 1.3 and 2.8 for the normalized coleoptile elongation and for the normalized K^+ conductance respectively. For K_{IC}*, the Ca^{2+} concentration causing half maximal inhibition of coleoptile elongation or inhibition of *G* (*see also* Eq. 1), values of 4.3 mM and of 1.2 mM were yielded respectively. The best fit was obtained with an integer Hill coefficient (*r*) of 1.

Discussion

The Inward Rectifier as Pathway for K^+ Uptake

In maize coleoptiles the plasma membrane of the cells of the outer epidermis and of the cortex cells contain a K^+ channel with a significant open probability only at negative *V*s. With an active proton ATPase in coleoptile cells, which polarizes the membrane, these channels can mediate passive K^+ influx. A stoichiometric (1:1) exchange of H^+ and K^+ measured in *Avena* coleoptile segments (Haschke & Lüttge 1973, 1975) renders this mechanism likely.

A parallel operation of a proton ATPase and an inward rectifying K^+ channel appears to be universal in plant cells for passive bulk K^+ uptake (reviewed in Schroeder, Ward, Gassmann, 1994). Accordingly, the K^+ inward rectifier found in the coleoptile protoplasts shares many qualitative similarities with K^+ inward rectifiers present in various other plant cells namely with respect to small single channel conductance, slow rising kinetics and sensitivities to extracellular TEA and $[Ca^{2+}]_o$ (reviewed in Schroeder et al., 1994).

The mean *V* of coleoptile protoplasts was positive of E_K but could in a few cases polarize well negative (maximum −120 mV) of all equilibrium voltages for passive ion distribution. These data point to the operation of a H^+-ATPase in the plasma membrane (*see also* Rück et al., 1993) which probably adds here to the apparent background currents.

Intact coleoptile cells from maize in solutions with 10 mM K^+ and 1 mM $[Ca^{2+}]_o$ display a *V* of −106 mV (*see also* Nelles & Müller, 1975) and hyperpolarize by approximately 10 mV in the presence of 10^{-5} M indole acetic acid (IAA) (Nelles & Müller, 1975). Further on, these two values (−106, and −116 mV) will be considered as ''characteristic'' *V* to estimate K^+ currents and fluxes at *V*s relevant for intact coleoptiles with and without auxin.

The measured $[Ca^{2+}]_o$ sensitive whole-cell K^+ inward current in coleoptile protoplasts at both voltages (±IAA) corresponds to net K^+ fluxes,

$$\Phi_K = I/F \qquad (3)$$

where *I* is the density of the membrane current and *F* the Faraday constant. The mean inward current in 10 mM external K^+ (I_{in} in 1 mM $[Ca^{2+}]_o$ minus background current I_{in} in 10 mM $[Ca^{2+}]_o$) measures 8 mA m^{-2} and 15 mA m^{-2} at −106 and −116 mV respectively. These K^+ currents convert to fluxes of 0.08 μmol m^{-2} sec^{-1} at −107 mV and about twice as much (0.16 μmol m^{-2} sec^{-1}) at −116 mV.

The net K^+ influx at −106 mV estimated from the mean currents at this voltage are approximately 6 times higher than those determined from ^{42}K tracer fluxes into auxin depleted *Avena* coleoptile tissue kept in 10 mM external K^+ (Pierce & Higinbotham, 1970). Thus, the conductance of the K^+ inward rectifier can account for the entire unidirectional K^+ tracer influx measured in grass coleoptiles. A plausible explanation for the 6-fold deviation between fluxes and currents is that fluxes were assayed (Pierce & Higinbotham, 1970) in the presence of high Mg^{2+} concentration (10 mM). Mg^{2+} may block the K^+ channels in a manner similar to Ca^{2+}.

K^+ Inward Rectifier and Coleoptile Elongation

In growing tissue cell elongation would decay if the turgor was not maintained by providing relevant amounts of

osmotic solutes (Cosgrove, 1986). The present data provide quantitative and pharmacological evidence for the hypothesis, that the K^+ inward rectifier is a main pathway for K^+ uptake during elongation and that the imported K^+ is crucial to maintain a turgor high enough to osmotically drive elongation.

First, the above-estimated doubling of unidirectional K^+ influx as a consequence of IAA-induced hyperpolarization roughly matches the 1.6-fold increase of net K^+ uptake into *Avena* coleoptiles in 10 mM external K^+ (Haschke & Lüttge, 1975). In this case, comparison of net influxes and unidirectional influxes is legitimate because of the small unidirectional efflux from expanding coleoptile cells. (Pierce & Higinbotham, 1970).

Main support for the idea that the K^+ inward rectifier is crucial for osmotic-driven elongation comes from the sensitivity of both cell elongation and K^+ conductance to $[Ca^{2+}]_o$ and TEA: The $[Ca^{2+}]_o$ sensitivity of the K^+ inward rectifier in coleoptile protoplasts can explain previous data which indirectly show a Ca^{2+}-induced inhibition of the K^+ conductance in intact coleoptile cells (Nelles & Müller, 1975; Nelles, 1976). In coleoptile tissue, a Nernstian response of V to extracellular K^+ in absence of $[Ca^{2+}]_o$ was decreased as $[Ca^{2+}]_o$ was increased (Nelles, 1976). On the background of the present data, the Nernstian voltage response in intact cells can readily be explained by the substantial K^+ conductance of the inward rectifier in the relevant voltage range. Furthermore, the measured decrease in conductance of the K^+ inward rectifier in response to elevated concentrations of $[Ca^{2+}]_o$ explains the sub Nernstian voltage response following elevation of $[Ca^{2+}]_o$ in coleoptile tissue. In conclusion, the electrical responses measured in coleoptile protoplasts reflect those obtained in intact coleoptile tissue. Thus, effects measured on the cellular level are likely to correspond to processes measured in the whole tissue.

The estimated $[Ca^{2+}]_o$ concentration for half maximal inhibition of coleoptile elongation and K^+ conductance differ by a factor of 4. This does not necessarily prove that the $[Ca^{2+}]_o$-evoked inhibition of the K^+ conductance is responsible for the inhibition of elongation. However, both K^+ conductance and elongation can also be inhibited by TEA, a monovalent cation, which bears no chemical similarities to Ca^{2+}.

Both results add up as conclusive evidence that the inward rectifier is a main pathway for K^+ uptake to drive elongation. An implication for the control of K^+-uptake is that the latter is under direct control of V. Thus, growth promoting hormones such as IAA and gibberellic acid can stimulate K^+-uptake under conditions of increased growth simply by their ability to polarize the membrane through stimulation of the H^+-ATPase activity (Nelles, 1977). However, a modulation of the K^+ inward rectifier in guard cells by auxins (Blatt & Thiel, 1994) implies additional control sites for K^+ uptake under hormonal control.

The data also show that the long-known inhibition of coleoptile elongation by extracellular Ca^{2+} (Cooil & Bonner, 1957; Tagawa & Bonner, 1957; Cleland & Rayle, 1977) can be understood — significantly if not mainly — by the sensitivity for the K^+ inward rectifier to Ca^{2+}. The difference between the estimated $[Ca^{2+}]_o$ concentrations for half maximal inhibition of K^+ conductance and elongation could have statistical reasons. But it can also be postulated that a $[Ca^{2+}]_o$ induced block of the inward rectifier causes a hyperpolarization of the membrane (Nelles & Müller, 1975) because of a decreased load of the pump. Hence, the inhibition of the K^+ conductance may partially be balanced by a concomitant increase in driving force. This could be the reason for the lower apparent $[Ca^{2+}]_o$ sensitivity to K^+ import.

Notably, the inhibition of the inward rectifier by $[Ca^{2+}]_o$ does not explain the entire Ca^{2+} sensitivity of coleoptile elongation. Although 10 mM $[Ca^{2+}]_o$ and 20 mM TEA completely block the inward rectifier, Ca^{2+} is significantly more potent as an inhibitor of elongation. It may therefore be concluded, that Ca^{2+} interferes in the intact tissue with additional processes that determine cell elongation (Cooil & Bonner, 1957; Cleland & Rayle, 1977). Furthermore, complete inhibition of the K^+ inward rectifier by TEA or $[Ca^{2+}]_o$ is not accompanied by complete block of elongation. Hence, cells must have additional mechanisms for the accumulation of osmotically active solutes (Rubinstein & Light, 1973; Haschke & Lüttge, 1975).

Tissue Specificity

The outer epidermis of coleoptiles has been suggested as the cell layer which *mechanically* limits growth of coleoptiles and exhibits a unique auxin sensitivity (Kutschera, Bergfeld & Schopfer, 1987). The present comparison of the inward rectifying K^+ channels in the plasma membrane of epidermis and cortex protoplasts bears no significant differences between cells from either tissue which would discriminate both cell types. Thus the data further add support to the notion, that a proposed prominent role of the outer epidermis is not related to the *electrical* properties of these cells as already proposed by Peters, Richter & Felle (1992).

Kinetics

The kinetic analysis of the voltage- and Ca^{2+}-controlled K^+ conductance renders the *parallel* model more likely to apply compared to either of the two serial models. In physiological terms, this result means that voltage and $[Ca^{2+}]_o$ act on the activity of the channel by independent modes. Whereas many K^+ channels in plants and fungi are blocked by $[Ca^{2+}]_o$ as a competing cation in a strik-

ingly cooperative mode with the voltage (Klieber & Gradmann, 1993, Bertl et al., 1993), this coupling seems to be weak in coleoptiles or even absent.

As for the absolute amounts of the rate constants k_I and k_A, which determine the velocity of the voltage-controlled activation/inactivation, Gradmann et al. (1993) have demonstrated — at least for guard cells — that plant cells with effective turgor control alternate appropriately between a state of ion uptake and a state of ion release, and that these switching kinetics are determined by the absolute rate constants of voltage-gated activation/inactivation. Correspondingly, coleoptiles under physiological conditions cannot be assumed to operate in a steady-state of ion uptake (where absolute rate constants are irrelevant), rather than in a sophisticated mode of turgor control when photo- and gravitropic growth responses are considered. In this context, determination of the absolute rate constants is important. One has to keep in mind, however, that these dynamic properties of ion channels can differ considerably depending on the physiological state of the membrane (e.g., in whole-cell measurements or in measurements with perforated patches, Oleson, De Felice & Donahoe, 1993). It would therefore, be premature to assign a physiological meaning to the absolute values of the rate constants determined under our experimental conditions.

On the other hand, the above comparison of measured steady-state K^+ currents and physiological K^+ uptake points to similar steady-state properties of the K^+ inward rectifier under experimental and physiological conditions. Under these circumstances, the model is expected to provide realistic estimates under physiological conditions with very low (<1 mM) external K^+ concentrations when K^+ uptake is hardly measurable.

Conclusions

Osmotically driven cell elongation in growing coleoptiles is inhibited by $[Ca^{2+}]_o$ via a voltage-independent Ca^{2+} block of voltage-gated K^+-channels that mediate substantial uptake of K^+.

This study was supported by grants of the Deutsche Forschugnsgemeinschaft (Gr 409/12–2, and Th 558/1–2).

References

Bertl, A., Slayman, C.L. 1990. Cation-selective channel in the vacuolar membrane of *Saccharomyces:* dependence on calcium, redox state, and voltage. *Proc. Natl. Acad. Sci. USA* **87:**7824–7828

Bertl, A., Slayman, C.L., Gradmann, D. 1993. Gating and conductance in an outward-rectifying K^+ channel from the plasma membrane of *Saccharomyces cerevisiae*. *J. Membrane Biol.* **132:**183–199

Blatt, M.R., Thiel, G. 1994. K^+ channels of stomatal guard cells: bimodal control of the K^+ inward-rectifier evoked by auxin. *The Plant Journal* **5:**55–68

Cleland, R.E., Rayle, D.L. 1977. Reevaluation of the effect of calcium ions on auxin-induced elongation. *Plant Physiol.* **60:**709–712

Cooil, B.J., Bonner, J. 1957. The nature of growth inhibition by calcium in the *Avena* coleoptile. *Planta* **48:**696–723

Cosgrove, D.J. 1986. Biophysical control of plant cell growth. *Annu. Rev. Plant Physiol.* **37:**377–405

Diekmann, W., Venis, M.A., Robinson, D.G. 1995. Auxins induce clustering of the auxin-binding protein at the surface of maize coleoptile protoplasts. *Proc. Natl. Acad. Sci. U.S.A.* (*in press*)

Föhr, K., Warchol, W., Gratzl, M. 1992. Calcium and control of free divalent cations in solutions used for membrane fusion studies. *Methods Enzymol.* **221:**149–157

Gradmann, D., Blatt, M.R., Thiel, G. 1993. Electrocoupling of ion transport in plants. *J. Membrane Biol.* **136:**327–332

Hamill, O.P., Marty, A., Neher, E., Sakmann, B., Sigworth, F.J. 1981. Improved patch-clamp techniques for high resolution current recording from cell and cell-free membrane patches. *Pfluegers Arch.* **391:**85–100

Haschke, H.-P., Lüttge, U. 1973. β-Indolylessigsäure-(IES)- abhängiger K^+-H^+-Austauschmechanismus und Streckungswachstum bei *Avena*-Koleoptilen. *Z. Naturforschung* **28:**555–558

Haschke, H.-P., Lüttge, U. 1975. Stoichiometric correlation of malate accumulation with auxin-dependent K^+-H^+ exchange and growth in *Avena* coleoptile segments. *Plant Physiol.* **56:**696–698

Hinchman, R.R. 1972. The ultrastructural morphology and ontogeny of oat coleoptile plastids. *Am. J. Bot.* **59:**805–817

Klieber, H.-G., Gradmann, D. 1993. Enzyme kinetics of the prime K^+ channel in the tonoplast of *Chara:* selectivity and inhibition. *J. Membrane Biol.* **132:**253–265

Kutschera, U., Bergfeld, R., Schopfer, P. 1987. Cooperation of epidermis and inner tissues in auxin-mediated growth of maize coleoptiles. *Planta* **170:**168–180

Neher, E. 1992. Correction for liquid junction potentials in patch clamp experiments. *Methods Enzymol.* **207:**123–130

Nelles, A. 1976. Das Membranpotential von Zellen der Maiskoleoptile unter dem Einfluß von Kalium- und Kalzium-Ionen. *Biochem. Physiol. Pflanzen* **169:**385–391

Nelles, A. 1977. Short-term effects of plant hormones on membrane potential and membrane permeability of dwarf maize coleoptile cells (*Zea mays* L. d_1) in comparison with growth responses. *Planta* **137:**293–298

Nelles, A., Müller, E. 1975. Ioneninduzierte Depolarisation der Zellen von Maiskoleoptilen unter dem Einfluß von Kalzium und β-Indolylessigsäure (IES). *Biochem. Physiol. Pflanzen* **167:**253–260

Oleson, D.R., DeFelice, L.J., Donahoe, R.M. 1993. A comparison of K^+ channel characteristics human T cells: perforated-patch versus whole-cell recording techniques. *J. Membrane Biol.* **132:**229–241

Peters, W., Richter, U., Felle, H. 1992. Auxin-induced H^+-pump stimulation does not depend on the presence of epidermal cells in corn coleoptiles. *Planta* **186:**313–316

Pierce, W.S., Higinbotham, N. 1970. Compartments and fluxes of K^+, Na^+ and Cl^- in *Avena* coleoptile cells. *Plant Physiol.* **46:**666–673

Robinson, R.A., Stokes, R.H. 1968. Electrolyte Solutions. Butterworth Scientific Publications, London

Rubinstein, B., Light, E.N. 1973. Indol acetic acid-enhanced chloride uptake into coleoptile cells. *Planta* **110:**43–56

Rück, A., Palme, K., Venis, M.A., Napier, R.M., Felle, H.H. 1993. Patch-clamp analysis establishes a role for an auxin binding protein in the auxin stimulation of plasma membrane currents in *Zea mays* protoplasts. *The Plant Journal* **4:**41–46

Schroeder, J.I., Ward, J.M., Gassmann, W. 1994. Perspectives on the physiology and structure of inward-rectifying K^+ channels in higher plants: Biophysical implications for K^+ uptake. *Annu. Rev. Biophys. Biomol. Struct.* **23:**441–471

Tagawa, T., Bonner, J. 1957. Mechanical properties of Avena coleoptile as related to auxin and to ionic interactions. *Plant Physiol.* **32:**207–212